JBC Papers in Press. Published on January 23, 2014 as Manuscript M113.515601
The latest version is at http://www.jbc.org/cgi/doi/10.1074/jbc.M113.515601

Retinoic acid receptor gamma (Rarg) and nuclear receptor subfamily 5, group A, member 2 (Nr5a2) promote conversion of fibroblasts to functional neurons

Zixiao Shi[1,2], Tianjin Shen[3], Yanli Liu[1], Yuanyuan Huang[1], Jianwei Jiao[1*]

[1]State Key Laboratory of Reproductive Biology, Institute of Zoology, Chinese Academy of Sciences, Beijing 100101, China; [2]University of Chinese Academy of Sciences, Beijing 100049, China; [3]School of Life Sciences, Anhui University, Anhui 230601, China.

Running title: *Rarg and Nr5a2 enhance fibroblasts convert into neurons*

[*]To whom correspondence should be addressed: Institute of Zoology, Chinese Academy of Sciences, Beijing 100101, China, Tel: 86-10-64806229, Email: jwjiao@ioz.ac.cn

Key words: adenovirus, fibroblast, neurons, nuclear receptors, retinoid

Background: It is necessary to identify more factors to increase fibroblast to neuron conversion efficiency with non-integration adenovirus.
Results: Nuclear receptor Rarg and Nr5a2 or agonist greatly enhance the conversion efficiency.
Conclusion: Rarg and Nr5a2 both promote transdifferentiation and improve neuronal function.
Significance: It would be of potential advantage to obtain safe and functional neurons with high efficiency.

ABSTRACT

Somatic cells can be reprogrammed to neurons and various other cell types with retrovirus or lentivirus. The limitation of this technology is that these genome-integration viruses may increase the risk of gene mutation and cause insertional mutagenesis. We recently found that non-integration adenovirus carrying neuronal transcription factors can induce fibroblasts to neurons. However, the conversion efficiency by the adenovirus is lower than that of the retrovirus or lentivirus. Therefore, it is crucial to identify other factors or chemical compounds to obtain neurons with high efficiency. In this study, we show that the combination of Rarg (RAR-γ) and Nr5a2 (also known as Lrh-1, liver receptor homologue 1) rapidly promote the iN cells maturation within one week and greatly facilitate the conversion with neuronal purities of approximately 50% and yields of more than 130%. They also improve neuronal pattern formation, electrophysiological characteristics and functional integration in vivo. Moreover, the

Downloaded from http://www.jbc.org/ by guest on April 28, 2020

Copyright 2014 by The American Society for Biochemistry and Molecular Biology, Inc.

chemical compound agonists to *Rarg* and *Nr5a2* function effectively as well. This approach may be used for the generation and application of iN cells in regenerative medicine.

The direct conversion of mouse and human fibroblasts (mesodermal lineage) to neurons (ectodermal lineage) (1,2) skips the neuronal differentiation processing from embryonic stem (ES) cells or induced pluripotent stem (iPS) cells, thereby providing the possibility of direct applications for clinical therapy. However, the direct transdifferentiation efficiency using a non-integrating system for iPS cells generation or other reprogramming is especially low (3,4). We previously found that the combination of Asc1, Brn2, and Ngn2 (ABN) could convert fibroblasts to neurons (5). However, the efficiency was not high using the adenoviral delivery system either. Therefore, we set out to increase the conversion efficiency by screening other transcription factors or small molecules in combination with ABN.

Retinoic acid (RA) plays an important role during neurogenesis in the central nervous system (CNS) of vertebrates (5-7), and RA is commonly used to promote neural stem cell differentiation into neurons in culture and in vivo (8,9). RA triggers neuronal differentiation through activating RA receptors (RARs), and various RARs-related downstream molecules have been reported to be involved in the process (10,11). RARs consist of three isoforms, RAR-α, RAR-β, and RAR-γ, which bind to both all-trans RA (atRA) and 9-cis RA (12,13). If RA signaling is disrupted, neurogenesis is affected, resulting in decreased numbers of newborn neurons (14,15). As RAR is important for neuronal differentiation, it is possible that RAR signaling could be beneficial for fibroblast-neuron trans-differentiation and could enhance the conversion efficiency. To validate this hypothesis, we overexpressed RARs or used RA agonists to explore the function of RARs in the conversion of fibroblasts to neurons.

Because RARs belong to the family of nuclear receptors which are important for differentiation and neurogenesis (8), it will be of interest to uncover other nuclear receptor members that could be used to enhance neuronal conversion. Recent studies showed that one important orphan nuclear receptor, *Nr5a2*, can enhance the reprogramming efficiency in the derivation of iPS cells (16,17). Therefore, we explored whether the nuclear receptors of *Nr5a2* together with *Rarg* enable efficiently convert fibroblasts to neurons. In this study, we used non-integrating adenoviruses carrying a different combination of transcription factors of ABN (*Ascl1*, *Brn2*, *Ngn2*), *Rarg*, and *Nr5a2* for the direct conversion of fibroblasts to functional neurons.

Here, we show that overexpression of *Rarg* or *Nr5a2* increases the fibroblast-to-neuron conversion efficiency. The combination of *Rarg* and *Nr5a2* could not only significantly promote the conversion efficiency but also improve the neuronal pattern formation and physiological function of induced neuron (iN) cells both in vitro and in vivo. Similarly, the chemical compound agonists to *Rarg* and *Nr5a2* work as effectively as the transcription

Downloaded from http://www.jbc.org/ by guest on April 28, 2020

factors. The strategy of using an adenoviral delivery system to obtain high iN cell conversion efficiency is promising and may be used as an improved tool for the application of iN cells in regenerative medicine.

EXPERIMENTAL PROCEDURES

Adenovirus production and infection— We used Invitrogen's Gateway Expression System to produce the adenovirus carrying the transcription factors *Ascl1, Brn2, Ngn2, Rarg,* and *Nr5a2*. The selected genes were amplified from a mouse cDNA library and inserted into the pEntr 3C vector (Invitrogen). According to the manufacturer's instructions, the resulting plasmids were generated by homologous L/R recombination. Then, viral constructs were transduced into a 293A cell line, and high titer (10^8 -10^{10} IU/ml) viral particles were obtained through two rounds of amplification. The adenoviral titer was determined using the same method as that of the lentiviral titer which takes advantage of 293T cells, except that the virus stock was diluted first because the high titer adenovirus could cause 293T cells to die quickly. Then, we used the adenovirus to infect mouse embryonic fibroblasts (MEFs) twice for 4 h per day at multiplicities of infection (MOI, number of viral particles per cell) of 10. Twenty-four hours post infection, half of the culture medium was changed into neural medium (Neural Basal/DMEM-F12 1:1, 1×B-27, 5 ng/ml BDNF) every day for two successive days. Next, half of the medium was changed every two days until the cells were ready for immunostaining and electrophysiological experiments. Chemical compounds were freshly added in neural medium when culture medium was changed.

Fibroblast isolation and culture— We used E13.5 C57BL/6 mouse embryos to isolate primary MEFs, as described previously [1]. The head, vertebral column, dorsal root ganglia, and visceral organs were removed, and then the remaining tissues were dissected into small pieces and digested for 10 minutes in 0.25% trypsin (Invitrogen). The dissociated cells were cultured in high glucose DMEM (Invitrogen), supplemented with 10% fetal bovine serum (FBS) (Biochrom), 0.1 mM non-essential amino acids (NEAA), and 2 mM Glutamax in a 37 ℃ and 5% CO2 incubator. The cells became confluent in approximately 2-3 days and were passaged in a 1:4 split. MEFs were used between passages 2 and 4.

Tail-tip fibroblasts (TTFs) were isolated from 6-week-old C57BL/6 mouse tail tips. The superficial dermis was peeled away, and the remaining tail tip was minced into 1-mm pieces. Two pieces were put into one gelatin-coated culture well of a 6-well plate; then, 2 ml of fibroblast culture medium was added, and the mixture was incubated at 37 ℃ for 5-7 d. Fibroblasts were collected until they migrated out of the tails and became fused; they were then passaged as MEFs.

Primary human embryonic fibroblasts (HEF) isolated from the epidermal tissue of 15-week-old fetus were obtained from Cell Resource Center, Institute of Basic Medical Sciences, Chinese Academy of Medical Sciences and Peking Union Medical College. HEF were cultured until the fibroblasts became fused, and digested by 0.25% trypsin and passaged

Downloaded from http://www.jbc.org/ by guest on April 28, 2020

in a 1:3 split in fibroblast medium.

Conversion efficiency— We counted the conversion efficiency by using the neuronal purity as the percentage of Tuj1 cells relative to the total final population (18). We randomly selected 8-10 visual fields for each well and calculated the total cell number visualized after DAPI staining and the total iN cell number indicated by Tuj1 staining. The efficiency was calculated by dividing the number of iN cells by the number of total cells in each visual field. We also calculated the neuronal yield as the percentage of Tuj1-positive cells relative to the initial population, as described previously (19).

Immunofluorescence— iN cells were fixed with 4% paraformaldehyde (PFA) in phosphate-buffered saline (PBS) for 20 min at room temperature and blocked with 5% BSA, 4% donkey serum, and 0.1% Triton X-100 for 30 min. Primary antibodies were diluted in antibody dilution solution (ADS, PBS with 1% BSA, 0.1% Triton X-100) in the following ratio, and secondary antibodies were diluted 1:1000 in ADS. iN cells were incubated in primary antibodies overnight at 4℃, and secondary antibodies were incubated for 60 min at room temperature. The following primary antibodies were used: rabbit anti-fibronectin (1:100, BOSTER), rabbit anti-S100A4 (FSP1) (1:100, Proteintech), mouse anti-GFAP (1:1000, Sigma), mouse anti-Nestin (1:200, Millipore), rabbit anti-Tuj1 (1:1,000, Sigma), mouse anti-Map2a (1:500, Millipore), mouse anti-NeuN (1:300, Millipore), mouse anti-synapsin (1:500, Synaptic Systems), rabbit anti-vGLUT1 (1:1000, Synaptic Systems), mouse anti-GAD67 (1:1000, Millipore), rabbite anti-TH (1:1000, Millipore), and DAPI (1:1,000, Sigma). Alexa Fluor 488- and Alexa Fluor 546-conjugated secondary antibodies were obtained from Invitrogen. Cy2-, Cy3- and Cy5-conjugated secondary antibodies were obtained from Jackson ImmunoResearch.

Transplantation of iN cells in vivo— iN cells were labeled with GFP by lentivirus infection, and approximately 10^5 cells were transplanted into the cortices of P6–10 pups (C57BL/6 background, ice anesthetized) or the brain dentate gyrus area (A/P: -2.0 mm, M/L: ±1.5 mm, D/V: -2.25 mm) of 6-week-old C57BL/6 mice (anesthetized with 70 mg/kg pentobarbital sodium). The mice were perfused with 0.9% saline, followed by 4% paraformaldehyde 1-4 weeks post-transplantation. The brains were dissected out and fixed in 4% paraformaldehyde overnight followed by dehydration in 0.1 M PBS containing 30% sucrose for 2 days at 4℃. Consecutive coronal sections (30 μm) were sliced using a Leica SM 2000R Sliding Microtome and stored in tissue collecting solution (25% glycerin, 25% ethylene glycol, in 0.1 M PBS) at −20°C until use.

Electrophysiology— MEF-derived iN cells were placed on glass coverslips for electrophysiological detection 7-12 days post infection. Whole-cell patch-clamp recordings in either voltage- or current-clamp mode were conducted to measure the voltage-activated sodium/potassium currents or action potentials, which were recorded using an Axopatch 200B or MultiClamp 700A amplifier (Molecular Devices). The electric signals were filtered at 2-10 kHz,

Downloaded from http://www.jbc.org/ by guest on April 28, 2020

digitized at 20-100 kHz (Digidata 1322A; Molecular Devices) and further analyzed using pClamp version 9.2 software (Molecular Devices). The intracellular fluid contained (in mM) 130 K^+-gluconate, 20 KCl, 10 HEPES, 0.2 EGTA, 4 Mg_2ATP, 0.3 Na_2GTP, and 10 Na^+-phosphocreatine (at pH 7.3, 310 mOsm), and the pipette ranged from 2.0-4.0 MΩ. The extracellular fluid consisted of (in mM) 124 NaCl, 3.3 KCl, 2.4 $MgSO_4$, 1.2 KH_2PO_4, 26 $NaHCO_3$, and 10 glucose (at pH 7.4, 310 mOsm). The transmitter receptor blockers, TTX (100 nM), AP5 (50 μM), and CNQX (10 μM), were used in the bath solution for the detection of action potentials and spontaneous excitatory postsynaptic currents (EPSCs).

Gene expression microarray analysis— Mouse genome-wide gene expression analysis was performed using Gene chips HOA 5.1 (Phalanx Biotech Group, Inc.). Total RNA was extracted from MEFs, ABN+*Rarg*+*Nr5a2* infected MEFs 12 days post infection and primary neurons which from hippocampus of postnatal day 0 (P0) C57BL/6 mouse (20); the total RNA was reverse transcribed using an Amino AllylMessageAmp™ II aRNA Amplification Kit (Ambion). For gene expression profiling analysis, mouse whole genome OneArray microarray v2 (MOA-002) chips were used with 26,423 mouse genome probes and 872 experimental control probes. Rosetta Resolver® System (Rosetta Biosoftware) was used to calculate the GeneChip Robust Multichip Average (GC-RMA) and normalize the datasets for single channel experiment analyses. Hierarchical clustering analysis was applied using a Euclidean distance matrix and the complete-linkage clustering method. Linear models and empirical Bayes methods were used to choose the differentially expressed genes that showed greater than two-fold changes and an adjusted P value less than 0.05.

PCR and Real-time PCR analysis— iN cells and wild-type neurons were cultured in neuron medium. MEFs were cultured in DMEM +10% FBS medium. All cells were washed with serum-free medium before collection. TRIzol extraction of total RNA was performed according to the manufacturer's instructions. Six hundred ng of total RNA was reverse transcribed and then quantified using SYBR Green (Tiangen), and β-actin was used as the reference.

NCAM1:
ATCCATTGACCGGGTGGAAC (F),
CGACTTCCACTCAGCCTTGT (R);
NCAM2:
TCTCTTGGTTCAGGAACGGC (F),
AGACATAAGAGCCCCCGTCT (R);
Tubb3:
GGGCGCATGTCTATGAAGGA (F),
TCACACACGGCTACCTTGAC (R);
Map2a:
AACCAATTCGCAGAGCAGGA (F),
GGGAGTTCCAGGGGTGATTG (R);
DCX:
TCAGGTAACGACCAAGACGC (F),
CAGACTTCCAGGGCTTGTGG (F);
NeuroD1:
CAGCTCAACCCTCGGACTTT (F),
GGGGACTGGTAGGAGTAGGG (R);
NeuroD2:
GTCCAAGATCGAGACCCTGC (F),
TGCACAGAGTCTGCACGTAG (R);
Zic1:
GGACACACACAGGGGAGAAG (F),
AAAGGTAGGGCTTGTCGCTC (R);
Brn4:

Downloaded from http://www.jbc.org/ by guest on April 28, 2020

CAGGGAGTTCCCAGCAATGG (F), CAGTTGCAGATCTTCGCGTC (R); *Myt1l*: AGCCATGTCAAAAAGCCATACT (F), TATCTTTGTGCGGGCATCCA (R); *NeuN*: GGCATGACCCTCTACACACC (F), TGTCTGTCTGTGCTGCTTCA (R); endo *Nr5a2*: ATCAGCAAGCAGGCAGAAGA (F), CTAGAGCAAGCTTCCAGGGG (R). *β-actin*: GGCTGTATTCCCCTCCATCG (F), CCAGTTGGTAACAATGCCATGT (R).

Genomic DNAs were purified from the adenovirus-infected MEFs and uninfected MEFs at 13-15 days post infection using the TIANamp Genomic DNA Kit (Tiangen). The templates were 50 ng genomic DNA and 1 pg vector for PCR. The following PCR protocol was set up as follows: 94 ℃ for 5 min, 30 repetitions of cycles at 94 ℃ for 30 s, 60 ℃ for 30 s, and 72 ℃ for 60 s or 120s, and finally 72 ℃ for 5 min. The forward primer was designed to recognize the pAD vector site, and the reverse primers were designed to recognize the DNA expression cassettes of *Ascl1*, *Brn2*, *Ngn2*, *Rarg* and *Nr5a2* respectively. pAD-F: TTAATACGACTCACTATAGGGA; *Ascl1*-R: ATAGAGTTCAAGTCGTTGGAGTAGT; *Brn2*-R: GTTGCTGTTGCTGTTGATGCT; *Ngn2*-R: CTTCGTGAGCTTGGCATCCT; *Rarg*-R: TCAGGGCCCCTGGTCAGGTT; *Nr5a2*-R: TTAGGCTCTTTTGGCATGCAGC; *GAPDH*-F: ATGGTGAAGGTCGGTGTGAACGGA; *GAPDH*-R: TTACTCCTTGGAGGCCATGTAGG.

Flow Cytometry Analysis— At 3 days post infection, cells of each group were dissociated into single cell suspensions for flow cytometry to analyze infection efficiency based on the ratio of GFP-positive cells. At 7 days post infection, cells were fixed with 4% PFA and stained with Tuj1 primary antibody and Cy5 secondary antibody to analyze neuronal conversion efficiency. Stained cells were analyzed by FACS Caliber apparatus (BD Biosciences) with FlowJo software (Tomy Digital Biology). The data were illustrated as percentage of total analyzed cells, which is the number of cells in each bin divided by the number of cells in the bin that contains the largest number of cells.

Statistical analysis— Statistical analysis was evaluated by two-tailed Student's t-tests. Values were considered statistically significant difference at $P<0.05$ (*), $P<0.01$ (**), and $P<0.001$ (***). Data are presented as mean ±SD or ± SEM in different experiments and all were described in the figure legends.

RESULTS

Rarg and Nr5a2 enhance transdifferentiation— Mouse embryonic fibroblasts (MEFs) were separated from E13.5 embryos and cultured as initial cells for neuronal conversion. MEFs showed classical fibroblasts morphology, and were positive for fibroblast markers including fibronectin and Fibroblast-specific protein 1 (FSP1, also called S100A4). No pre-existing neurons, astrocytes or neural progenitor cells were detected in the culture of the MEFs,

Downloaded from http://www.jbc.org/ by guest on April 28, 2020

as demonstrated by immunocytochemistry with specific markers such as Tuj1, NeuN, GFAP, and Nestin (data not shown). The mouse cDNAs of *Ascl1*, *Brn2*, *Ngn2*, *Rarg*, and *Nr5a2* were carried by a modified commercial adenoviral vector (Invitrogen, pAd/CMV/V5-DEST) under the CMV promoter. The MEFs were infected once a day for two consecutive days (Fig. 1*A*) with several groups of adenoviruses carrying the genes for *GFP*, ABN, ABN+*Rarg*, ABN+*Nr5a2*, and ABN+*Rarg*+*Nr5a2* (Fig. 1*B*-1*G*).

We counted the conversion efficiency by calculating the neuronal purity as the percentage of Tuj1 cells relative to the final population 7 days post infection. We also calculated the neuronal yield as the percentage of Tuj1-positive cells relative to the initial population, as described in methods and previously used by other lab (1). Because RA signaling through RA receptor is necessary for neurogenesis and neural development, we applied *Rarg* into the three-factor combination of ABN. Three days post infection, the infected MEFs appeared to show neuronal morphology with thin processes due to the addition of *Rarg* into ABN. Seven days later, more mature neuronal cells with Tuj1-positive staining were clearly detected, and the neuronal purity ratio became 10.83±2.67% (Fig. 1*B*, 1*C*). Considering the important role of RA signaling, we subsequently studied whether RA could enhance the conversion. The results showed RA could intensively promote iN cell conversion when it was added to the culture medium, and we found that atRA at a concentration of 0.5 μM had the highest effect. Thus, neural medium used in the afterward experiments was all supplemented with atRA.

Recently, miRNAs were shown to be involved in the conversion of fibroblasts to neurons (21,22). Other nuclear receptors, such as *Nr5a2*, also participate in cell reprogramming (16,17). Therefore, we performed studies to investigate whether these factors enhance the conversion in our system. After extensive screening, *Nr5a2* was identified to be a good candidate to significantly enhance the conversion efficiency. The synergistic addition of *Rarg* and *Nr5a2* with ABN greatly boosted the neuronal purity efficiency to 44.33±4.25% and increased the neuronal yields to 131.48±16.38% (Fig. 1*H*), showing a more than 10-fold enhancement compared with ABN alone (Fig. 1*D*, 1*E*). The synergistic contribution of *Rarg* and *Nr5a2* suggests that they could activate different signaling pathways to enhance the direct conversion of fibroblasts to neurons.

To check whether adenoviral integration occured in genome in this experiment, PCR analysis was performed using genomic DNA from uninfected MEFs, MEFs infected with control-GFP and MEFs infected with the ABN+*Rarg*+*Nr5a2* combination. No predicted PCR-amplified band was observed in any of the samples except in the positive control lane. GAPDH was simultaneously amplified as an internal control (data not shown).

We observed that the ABN+*Rarg*+*Nr5a2* iN cells showed extremely abundant nerve neurites and synaptic connections at a very early stage (3-4 days post infection). To further analyze the fast and efficient

Downloaded from http://www.jbc.org/ by guest on April 28, 2020

effect of *Rarg* and *Nr5a2*, we stained cells with a marker for relatively mature neurons, Map2a, to trace the appearance of neuronal cells over time. ABN+*Rarg*+*Nr5a2* only required 3 days to obtain Map2a-positive neuronal cells, and this conversion period was shortened two-fold relative to ABN alone (Fig. 1*I*).

Conversion with chemical compound agonists— Chemical approaches to manipulate biological systems have been proven to be powerful tools for studying reprogramming (23). It is advantageous to identify chemical compounds to replace transcription factors for converting fibroblasts to neurons. In this study, CD437 (6-[3-1-Adamantyl)-4-hydroxyphenyl]-2-naphthalene carboxylic acid), a specific Rarg agonist (24), and DLPC (1,2-dilauroylglycero-3-phosphocholine), an Nr5a2 agonist (25), were chosen to investigate whether these small molecules could substitute or partially substitute the corresponding transcription factors. We not only found that MEF expressed *Nr5a2*, but also detected DLPC increased endogenous *Nr5a2* expression in our transdifferentiation system (data not shown). Applying the specific RA agonist CD437 to *Rarg* could enhance the conversion from MEFs and had a consistent effect as that of *Rarg*. Moreover, the combination of the DLPC and CD437 increased the conversion efficiency by approximately 2-fold (Fig. 1*F*, 1*G*).

The conversion efficiency was also greatly enhanced when both the *Rarg* agonist CD437 and the *Nr5a2* agonist DLPC were applied to the culture medium, and the result was quite favorable (Fig. 1*F*, 1*G*). The effect of the agonists was dose-dependent on an effective concentration of CD437 at 0.1 μM and DLPC at 2 μM. The two chemical compound agonists synergistically functioned together to drive the neuronal purity efficiency to 37.83±4.17 and the neuronal yields to 127.82±21.64%; these values did not significantly differ from those for the transcription factors (Fig. 1*F*, 1*H*).

In order to analyze the infection efficiency and conversion efficiency more accurately, we used flow cytometry to analyze the efficiencies. At 3 days post infection, GFP-positive cells ratio of the three groups of ABN, ABN+CD437+DLPC, and ABN+*Rarg*+*Nr5a2* was similar, which was among the range of 77.9% to 85.1%. At 7 days post infection, the ratio of Tuj1-positive cells in relative to total cells was calculated as conversion efficiency. The efficiencies were 1.94% for ABN, 40.8% for ABN+CD437+DLPC, and 46.2% for ABN+*Rarg*+*Nr5a2* (data not shown). The iN cell conversion from MEFs by the chemical compound agonists was consistent to that by the transcription factors of *Rarg* and *Nr5a2*.

Rarg and Nr5a2 or chemical compounds facilitate neuronal maturity— To further analyze the chemical compound effects, we examined the iN cell morphology and the expression of several specific neuronal markers in different stages of conversion. Tuj1-positive cells appeared quite early and the morphology became extremely complex within 5 days due to the addition of *Rarg* and *Nr5a2* or the chemical compound agonists. Compared

Downloaded from http://www.jbc.org/ by guest on April 28, 2020

with ABN iN cells, *Rarg*- and *Nr5a2*- or chemical compound-activated iN cells exhibited much more elaborate dendrites at one or two weeks post infection, indicating that *Rarg* and *Nr5a2* or the agonists induced neurons more maturity (Fig. 2*A*, 2*E*). *Rarg* and *Nr5a2* increased the ratio of multipolar neuronal cells to approximately 50% (Fig. 2*B*) and also significantly boosted the total dendritic length and the branch numbers (Fig. 2*C*, 2*D*) at one week post infection. The cumulative distribution analysis of the dendritic arborization further demonstrated an increase in dendritic complexity enhanced by *Rarg* and *Nr5a2* or by the chemical compound agonists (Fig. 2*F*-*G*) at two weeks post infection. Thus, activated *Rarg* and *Nr5a2* accelerate the dendritic development of iN cells.

Next, to determine whether *Rarg* and *Nr5a2* could enhance iN cell maturation in electrophysiological characteristics, we detected the action potentials of those iN cells every day beginning 5 days post infection. As early as 5 days post infection, *Rarg*- and *Nr5a2*-activated iN cells could exhibit action potentials, and at 7 days post infection, iN cells exhibited repetitive action potentials which indicated neuronal maturation. At 7 days post infection, we compared some electrophysiological parameters between the *Rarg*- and *Nr5a2*-activated and the ABN groups. *Rarg* and *Nr5a2* or chemical compounds acutely facilitated the increase in K^+ and Na^+ currents (Fig. 3*A*, 3*C*, 3*D*) and the activity of action potentials (Fig. 3*B*) in induced neurons. By step-depolarizing the membrane in the current-clamp mode, almost all of the *Rarg*- and *Nr5a2*-activated iN cells could elicit single or multiple action potentials, and the majority of the cells fired repetitive action potentials (19 out of 20 for the ABN+CD437+DLPC group and 24 out of 26 for the ABN+*Rarg*+*Nr5a2* group) (Fig. 3*E*). The ratio of cells evoking action potentials was much higher in the *Rarg*- and *Nr5a2*-activated iN cells than that in the ABN iN cells, which showed a ratio of 4 out of 14 cells. Other electrophysiological parameters, such as action potential height, resting membrane potential, membrane input resistance, and membrane capacitance, also showed *Rarg* and *Nr5a2* promote iN cells maturation (Fig. 3*F*-3*H*).

Characterization of Rarg- and Nr5a2-activated iN cells— The ABN+*Rarg*+*Nr5a2* converted iN cells were positive for Tuj1 with highly complex neuronal morphology, and these cells also expressed specific neuronal markers, Map2a, NeuN, and synapsin, seven days post infection (Fig. 4*A*-*C*). The chemical compound agonist-converted iN cells also expressed the pan-neuronal markers (data not shown).

To study the specific neuron phenotypes of ABN+*Rarg*+*Nr5a2* iN cells, immunohistochemistry was performed on cells infected for a longer cultivation time of approximately two weeks. The majority of Tuj1-positive cells were distinctly positive for vGLUT1 (69.2±15.6% of Tuj1-positive cells), and a much smaller fraction of the neurons were positively labeled for GAD67 (5.5±4.7% of Tuj1-positive cells) (Fig. 4*D*, 4*E*). Occasionally, tyrosine hydroxylase-positive cells were detected (Fig. 4*F*). An analogous phenomenon

Downloaded from http://www.jbc.org/ by guest on April 28, 2020

was observed in chemical compound agonist-treated ABN iN cells (data not shown).

To further investigate the synaptic connections between cells, we detected the spontaneous postsynaptic currents (PSC) electrophysiological activity of *Rarg*- and *Nr5a2*-activated iN cells with neuronal morphology. After being cultured in neuron medium for 12-14 days, *Rarg*- and *Nr5a2*-activated iN cells continued to display full-blown and stable action potentials (Fig. 4*G*, 4*L*) and Na^+/K^+ currents (Fig. 4*H*, 4*M*) and frequently expressed synapsin (Fig. 4*J*, 4*O*). Furthermore, iN cells could show spontaneous synaptic activity with each other without needing to be co-cultured with primary neurons (Fig. 4*I*, 4 *K*, 4*N*, 4*P*). The recorded iN cells (19 out of 22 of the ABN+CD437+DLPC group and 16 out of 18 of the ABN+*Rarg*+*Nr5a2* group) showed PSCs, which indicated that iN cells were capable of forming synapses with surrounding cells. The majority spontaneous postsynaptic currents could be greatly blocked by the presence of a blocker combination of CNQX (6-cyano-7-nitroquinoxaline-2,3-dione, AMPA/kainate receptor antagonist) and AP5 ((2R)-amino-5-phosphonovaleric acid, NMDA receptor antagonist) (data not shown), further indicating that the recorded PSCs were mainly EPSCs. The electrophysiological data also suggested that *Rarg*-and *Nr5a2*-activated iN cells not only had higher conversion efficiency but also showed better physiological function. The most important point is that *Rarg* and *Nr5a2* intensely promoted rapid maturation of the induced neurons.

Other electrophysiological parameters were measured in voltage-clamp mode. Step depolarization induced the opening of voltage-dependent sodium and potassium ion channels, which correspond to the fast and inactivating inward sodium currents and the outward potassium currents, respectively, with a possible contribution from calcium currents to the whole-cell currents (Fig. 4). The action potentials and the fast and transient inward sodium currents were blocked by tetrodotoxin (TTX), a specific inhibitor of sodium ion channels (data not shown).

Rarg and Nr5a2 also promote adult mouse fibroblast and human fibroblast conversion— To determine whether *Rarg* and *Nr5a2* could also promote iN cell conversion from adult mouse and human fibroblasts, TTFs were isolated from 6-week-old C57BL/6 mice, and HEFs were isolated from 15-week-old human foreskin tissue. TTFs and HEFs were detected to be fibronectin-positive and Tuj1/GFAP/nestin-negative (data not shown). Tuj1- positive TTF-iN cells were observed 4 days post infection, and Tuj1- positive HEF-iN cells were observed 7 days post infection. The neuronal conversion efficiencies from TTFs and HEFs were lower than that from MEFs, which is consistent to previous report (2). TTF-iN cells and HEF-iN cells also expressed the pan-neuronal markers Map2a, NeuN, and synapsin (Fig. 5*A*-*F*) 10-13 days post infection and demonstrated the electrophysiological signals of action potentials, sodium currents, and potassium currents (Fig. 5*G*-*J*) 15 days post infection. However, iN cells converted from human fibroblasts using ABN alone required 20-30 days to

Downloaded from http://www.jbc.org/ by guest on April 28, 2020

become sufficiently mature to fire action potentials (data not shown). The data indicate that Rarg and Nr5a2 can promote iN cell conversion not only from mouse fibroblasts but also from human fibroblasts.

In vivo analysis of iN cells after transplantation— Furthermore, we investigated the iN cell conversion, survival, and function integration after transplanting infected MEF cells to the adult hippocampal area. To trace the transplanted cells in the brain, we first infected MEFs with a lentivirus that stably expressed GFP, then with adenoviral ABN+*Rarg*+*Nr5a2*. Three days post infection, the cells were transplanted into the cortices of P6–10 pups (C57BL/6 background) (Fig. 6*A*-*D*) or the dentate gyrus (DG) (a native neurogenesis area in the adult mouse brain) of the hippocampus of 6-week-old C57BL/6 mice (Fig. 6*E*-*H*). The mice, which received grafts bilaterally, were euthanized 1-4 weeks after transplantation, and the brain sections were collected for analysis. The donor cells that showed GFP fluorescence were restricted to the injection site within the cortex or DG (Fig. 6*A*, 6*E*). The transplanted cells also swiftly converted into neurons in vivo. Within 1 week after transplantation, DCX-positive cells labeled with GFP were detected (Fig. 6*B*, 6*F*), suggesting that the MEF cells were successfully converted into neurons in vivo. Furthermore, the iN cells matured soon in vivo, and NeuN-positive cells were detected 2 weeks following transplantation (Fig. 6*C*, 6*G*). To explore whether the grafted cells could establish functional connections with host neurons, we stained the sections with synapsin 2-4 weeks post-transplantation, and the data indicated that some grafted cells had received extensive presynaptic innervation from other neurons within two weeks (Fig. 6*D*, 6*H*). The iN cells were postmitotic; therefore, they theoretically did not possess oncogenicity. For 4-6 months following transplantation of iN cells in more than 30 mice, we did not observe tumor formation, indicating the safety of using iN cells in vivo and the potential of these cells as a source for cell replacement therapy.

Global gene expression and real-time PCR detection of ABN+Rarg+Nr5a2 iN cells— To explore more details in the similarities and differences between ABN+*Rarg*+*Nr5a2* iN cells and primary neurons, we compared the global gene expression pattern of matured iN cells 12 days post infection with mouse primary neurons and MEFs by microarray analysis. Cells for the array experiment were the total final cells population including converted iN cells and non-converted cells and formed a mixed population. The mixed population might reflect the actual changes in gene expression levels compared with those in MEFs because Tuj1-negative cells could be partially converted cells and present some neuron-specific genes in addition to those of Tuj1-positive iN cells. Hierarchical clustering revealed that the global gene expression profile of iN cells showed a higher degree of similarity to primary neurons than to MEF cells. Among 4384 differentially regulated genes with a more than two-fold change between primary

Downloaded from http://www.jbc.org/ by guest on April 28, 2020

neurons and MEFs, and 2587 genes were downregulated or upregulated in the exact same manner between iN cells and MEFs. The others were almost classified in the same family and possessed analogous function between the two groups (Fig. 7*A*).

In iN cells, functionally categorized genes associated with neurogenesis, synaptic transmission, and axonogenesis were upregulated; examples include NCAM, Dcx, Neurod, Sox2, Syap1, Snca, Ncald, Negr1, Npy, and Myt1l (Fig. 7*B*). Functional categorized genes associated with fibroblast activity and mitosis were downregulated (Fig. 7*B*). For instance, fibroblast growth factor 5 was completely undetected in iN cells and neurons, which indicated that even the mixture of conversion cells had lost their initial nature and turned to the other state. We also highlighted the genes listed under the GO (Gene Ontology) biological process category neurogenesis during neural development and differentiation. Additionally, indicated by the micorarry results, *Rarg* activated retinoic acid signaling pathway members, such as CRABP, PPAR-gamma, and CYP2D22, which participate in neuronal differentiation or survival. *Nr5a2* also up-regulated many neural metabolism process or transition associated molecules, such as NSMCE2, RANBP9, and CHEK. The data discussed in this publication have been deposited in NCBI's Gene Expression Omnibus (Jiao J *et al*., 2013) and are accessible through GEO Series accession number GSE52993 (http://www.ncbi.nlm.nih.gov/geo/query/acc.cgi?acc=GSE52993).

Subsequently, we selected some neuron specificity genes to examine their relative expression level using real-time fluorescence quantitative PCR in MEFs, ABN+*Rarg*+*Nr5a2* iN cells, and primary neurons. The data show that those neuron-specific genes were upregulated in iN cells compared with the expression in MEFs, and the most changed gene was escalated more than 50-fold (Fig. 7*C*). The upregulated tendency was identical for primary neurons and MEFs, which is consistent to the change from microarray analysis.

DISCUSSION

Research on transdifferentiation or transdetermination can be traced back to 1980s, when transient expression of DNA prepared from specific primary cells or cell lines could transform or induce differentiation of the recipient cells (26). Since then, scientists began to explore the effects of ectopic specific genes expression or re-activation of endogenous genes during transdifferentiation process.

Virus-mediated gene transfer offers more advantages over DNA/RNA-mediated gene delivery, especially in the comparatively long term expression of the introduced genes. Therefore, retrovirus, lentivirus, or adenovirus mediated gene delivery system has been widely used in the scientific field of committed differentiation and embryonic development.

It was firstly reported that functional neurons could be directly generated from mouse primary fibroblasts through ectopic expression of three transcriptional factors (1). Subsequently, functional specific neurons such as dopaminergic neurons were also successfully reprogrammed from both

Downloaded from http://www.jbc.org/ by guest on April 28, 2020

mouse and human fibroblasts (27). However, all these breakthroughs depend on the integrating lenti/retroviral system, which is known to increase the risk of insertional mutagenesis. We previous found that adenovirus transiently expressing Ascl1, Brn2, and Ngn2 can convert fibroblasts to neurons (18). However the induction efficiency is low, therefore it is ideal to identify other factors to obtain high conversion efficiency.

In this study, we used adenoviruses carrying a different combination of transcription factors of Rarg and Nr5a2 with ABN for the conversion of mouse embryonic and adult fibroblasts to neurons, as well as human fibroblasts. We successfully rapidly converted fibroblasts to neurons with ABN+*Rarg*+*Nr5a2* factors, and chemical compounds agonists could replace some of those factors. Our data showed that the combination of Rarg and Nr5a2 could produce an enhanced effect during conversion, indicating that RA signaling functioned synergistically with Nr5a2 to mediate the transdifferentiation. It has been demonstrated that the factors of Rarg and Nr5a2 could enhance reprogram fibroblasts to iPS cells (17). The possible mechanism as they explained is that these two factors may bind to key pluripotency genomic loci and promote activation of these genes. In our study, Rarg and Nr5a2 may act differently as general modulator of neural related genes, since at least RA signaling with important roles in brain has been widely studied in neural regulation (5) and Nr5a2 is also expressed in the brain (28). However, we could not exclude the other possibility that these two factors partially reprogram fibroblasts after activate pluriotency genes. Then, the neural-specific transcription factors and neuronal medium further promote fibroblasts to neurons.

The iN cells showed neuronal morphology and neuronal gene expression patterns, generated action potentials, and formed synaptic connections. The data indicated that the iN cells mature much more rapidly and are functionally homoplastic to primary neurons. The iN cells could survive more than one month after the transgenes were silenced in vitro. The adenoviral integration free system and the small molecule protocol for neuronal conversion would broaden the application of iN cells. Future studies are required to study the molecular mechanism of converting fibroblasts to neurons and to study the functions of iN cells in vivo. Moreover, it will be of interest to obtain iN cells of specific neuronal subtypes from fibroblasts. The data from the small molecule treatment indicated that RA signaling and *Nr5a2* had important roles during the neuronal conversion. The strategy of including chemical compounds would ultimately be beneficial and promising for cell therapy and clinical applications. In conclusion, safe and functional iN cells that require less time to mature and gain higher efficiency would have potential in regenerative clinical applications. Adenoviral transduction may be used as an improved tool for the application of iN cells in regenerative medicine.

Downloaded from http://www.jbc.org/ by guest on April 28, 2020

REFERENCES

1. Vierbuchen, T., Ostermeier, A., Pang, Z. P., Kokubu, Y., Sudhof, T. C., and Wernig, M. (2010) Direct conversion of fibroblasts to functional neurons by defined factors. *Nature* **463**, 1035-1041
2. Pang, Z. P., Yang, N., Vierbuchen, T., Ostermeier, A., Fuentes, D. R., Yang, T. Q., Citri, A., Sebastiano, V., Marro, S., Sudhof, T. C., and Wernig, M. (2011) Induction of human neuronal cells by defined transcription factors. *Nature* **476**, 220-223
3. Stadtfeld, M., Nagaya, M., Utikal, J., Weir, G., and Hochedlinger, K. (2008) Induced pluripotent stem cells generated without viral integration. *Science* **322**, 945-949
4. Zhou, W., and Freed, C. R. (2009) Adenoviral gene delivery can reprogram human fibroblasts to induced pluripotent stem cells. *Stem Cells* **27**, 2667-2674
5. Maden, M. (2002) Retinoid signalling in the development of the central nervous system. *Nature reviews. Neuroscience* **3**, 843-853
6. Lane, M. A., and Bailey, S. J. (2005) Role of retinoid signalling in the adult brain. *Progress in neurobiology* **75**, 275-293
7. Zechel, C. (2005) Requirement of retinoic acid receptor isotypes alpha, beta, and gamma during the initial steps of neural differentiation of PCC7 cells. *Mol Endocrinol* **19**, 1629-1645
8. Jacobs, S., Lie, D. C., DeCicco, K. L., Shi, Y., DeLuca, L. M., Gage, F. H., and Evans, R. M. (2006) Retinoic acid is required early during adult neurogenesis in the dentate gyrus. *Proceedings of the National Academy of Sciences of the United States of America* **103**, 3902-3907
9. Rhinn, M., and Dolle, P. (2012) Retinoic acid signalling during development. *Development* **139**, 843-858
10. Lu, J., Tan, L., Li, P., Gao, H., Fang, B., Ye, S., Geng, Z., Zheng, P., and Song, H. (2009) All-trans retinoic acid promotes neural lineage entry by pluripotent embryonic stem cells via multiple pathways. *BMC cell biology* **10**, 57
11. McCaffery, P., Zhang, J., and Crandall, J. E. (2006) Retinoic acid signaling and function in the adult hippocampus. *Journal of neurobiology* **66**, 780-791
12. Giguere, V., Ong, E. S., Segui, P., and Evans, R. M. (1987) Identification of a receptor for the morphogen retinoic acid. *Nature* **330**, 624-629
13. Drager, U. C. (2006) Retinoic acid signaling in the functioning brain. *Science's STKE : signal transduction knowledge environment* **2006**, pe10
14. Boylan, J. F., Lufkin, T., Achkar, C. C., Taneja, R., Chambon, P., and Gudas, L. J. (1995) Targeted disruption of retinoic acid receptor alpha (RAR alpha) and RAR gamma results in receptor-specific alterations in retinoic acid-mediated differentiation and retinoic acid metabolism. *Molecular and cellular biology* **15**, 843-851
15. Luo, T., Wagner, E., Crandall, J. E., and Drager, U. C. (2004) A retinoic-acid critical period in the early postnatal mouse brain. *Biological psychiatry* **56**, 971-980
16. Heng, J. C., Feng, B., Han, J., Jiang, J., Kraus, P., Ng, J. H., Orlov, Y. L., Huss, M., Yang, L.,

Downloaded from http://www.jbc.org/ by guest on April 28, 2020

Lufkin, T., Lim, B., and Ng, H. H. (2010) The nuclear receptor Nr5a2 can replace Oct4 in the reprogramming of murine somatic cells to pluripotent cells. *Cell stem cell* **6**, 167-174

17. Wang, W., Yang, J., Liu, H., Lu, D., Chen, X., Zenonos, Z., Campos, L. S., Rad, R., Guo, G., Zhang, S., Bradley, A., and Liu, P. (2011) Rapid and efficient reprogramming of somatic cells to induced pluripotent stem cells by retinoic acid receptor gamma and liver receptor homolog 1. *Proceedings of the National Academy of Sciences of the United States of America* **108**, 18283-18288
18. Meng, F., Chen, S., Miao, Q., Zhou, K., Lao, Q., Zhang, X., Guo, W., and Jiao, J. (2012) Induction of fibroblasts to neurons through adenoviral gene delivery. *Cell research* **22**, 436-440
19. Ladewig, J., Mertens, J., Kesavan, J., Doerr, J., Poppe, D., Glaue, F., Herms, S., Wernet, P., Kogler, G., Muller, F. J., Koch, P., and Brustle, O. (2012) Small molecules enable highly efficient neuronal conversion of human fibroblasts. *Nature methods* **9**, 575-578
20. Banker, G., and Goslin, K. (1998) *Culturing nerve cells*, 2nd ed., MIT Press, Cambridge, Mass.
21. Yoo, A. S., Sun, A. X., Li, L., Shcheglovitov, A., Portmann, T., Li, Y., Lee-Messer, C., Dolmetsch, R. E., Tsien, R. W., and Crabtree, G. R. (2011) MicroRNA-mediated conversion of human fibroblasts to neurons. *Nature* **476**, 228-231
22. Ambasudhan, R., Talantova, M., Coleman, R., Yuan, X., Zhu, S., Lipton, S. A., and Ding, S. (2011) Direct reprogramming of adult human fibroblasts to functional neurons under defined conditions. *Cell stem cell* **9**, 113-118
23. Li, W., Jiang, K., Wei, W., Shi, Y., and Ding, S. (2013) Chemical approaches to studying stem cell biology. *Cell Res* **23**, 81-91
24. Gianni, M., Zanotta, S., Terao, M., Garattini, S., and Garattini, E. (1993) Effects of synthetic retinoids and retinoic acid isomers on the expression of alkaline phosphatase in F9 teratocarcinoma cells. *Biochemical and biophysical research communications* **196**, 252-259
25. Lee, J. M., Lee, Y. K., Mamrosh, J. L., Busby, S. A., Griffin, P. R., Pathak, M. C., Ortlund, E. A., and Moore, D. D. (2011) A nuclear-receptor-dependent phosphatidylcholine pathway with antidiabetic effects. *Nature* **474**, 506-510
26. Davis, R. L., Weintraub, H., and Lassar, A. B. (1987) Expression of a single transfected cDNA converts fibroblasts to myoblasts. *Cell* **51**, 987-1000
27. Caiazzo, M., Dell'Anno, M. T., Dvoretskova, E., Lazarevic, D., Taverna, S., Leo, D., Sotnikova, T. D., Menegon, A., Roncaglia, P., Colciago, G., Russo, G., Carninci, P., Pezzoli, G., Gainetdinov, R. R., Gustincich, S., Dityatev, A., and Broccoli, V. (2011) Direct generation of functional dopaminergic neurons from mouse and human fibroblasts. *Nature* **476**, 224-227
28. Grgurevic, N., Tobet, S., and Majdic, G. (2005) Widespread expression of liver receptor homolog 1 in mouse brain. *Neuro endocrinology letters* **26**, 541-547

Downloaded from http://www.jbc.org/ by guest on April 28, 2020

ACKNOWLEDGMENTS—We are grateful to Dangsheng Li, Qi Zhou, and Baoyang Hu for critical comment and discussion; members of the Jiao lab for discussion; Shiwen Li for technical assistance.

FOOTNONTES

*This work was supported by the National Basic Research Program of China (2014CBCB964903), the National Science Foundation of China (31371477), the Strategic Priority Stem Cell Program (XDA01020301), and the Hundreds Talent Program.

To whom correspondence should be addressed: Institute of Zoology, Chinese Academy of Sciences, Beijing 100101, China, Tel: 86-10-64806229, Email: jwjiao@ioz.ac.cn

The abbreviations used are: ABN, *Ascl1+Brn2+Ngn2*; RA, retinoic acid; RARs, RA receptors; Rarg, RA receptor-γ; Nr5a2, nuclear receptor subfamily 5, group A, member 2; iN, induced neuron; ES cells, embryonic stem cells; iPS cells, induced pluripotent stem cells; CNS, central nervous system; MOI, number of viral particles per cell; MEFs, mouse embryonic fibroblasts; AP, action potential; Cm, membrane capacitance; Rs, membrane series resistances; RMP, resting membrane potential; PSCs, spontaneous postsynaptic currents; EPSCs, excitatory spontaneous postsynaptic currents; TTX, tetrodotoxin; CNQX, 6-cyano-7-nitroquinoxaline-2,3-dione; AP5, (2R)-amino-5-phosphonovaleric acid. CD437, 6-[3-(1-Adamantyl)-4-hydroxyphenyl]-2-naphthalene carboxylic acid; DLPC, 1,2-dilauroylglycero-3-phosphocholine.

Downloaded from http://www.jbc.org/ by guest on April 28, 2020

FIGURE LEGENDS

FIGURE 1. Generation of iN cells by the combination of the nuclear receptors *Rarg* and *Nr5a2* as well as chemical compound agonists. *A*. Diagram depicting the procedures for transdifferentiation of MEFs to neurons by adenoviruses carrying ABN+*Rarg*+*Nr5a2*. *B, C*. RA signaling and *Rarg* enhance neuronal conversion, which was estimated by neuronal purity (Tuj1 cells to final total cells). Tuj1 staining was performed 7 days post-infection for MEFs infected with the corresponding adenovirus. *D, E*. Nuclear receptor *Nr5a2* promotes neuronal conversion. The combination of *Rarg* and *Nr5a2* greatly enhance neuronal conversion from fibroblasts. ABN+*Rarg*+*Nr5a2* iN cells show highly complex neuronal morphologies and higher efficiency. iN cells were stained with Tuj1 and quantified 7 days post infection. *F, G*. Chemical compound agonists of *Rarg* and *Nr5a2* effectively enhance conversion. The efficiencies were calculated for the conversion of MEFs to neurons with ABN, CD437 (*Rarg* agonist), and DLPC (*Nr5a2* agonist) independently or in combination. *H*. Quantification of neuronal yields (Tuj1 cells to initial plated cells; 100%: the number of Tuj1 cells equal to initial cells) 7 days post infection. *I*. The kinetics of transdifferentiation using different combinations. MEFs were treated with different combinations, and the Map2a fluorescence was detected every 12 hr. The green bars indicate the emergence of GFP-positive cells, whereas the yellow bars indicate the presence of both GFP-positive and Map2a-positive cells. Two representative independent experimental sets are shown. GFP viruses were used as the control. The data are presented as the mean ± SD of cell counts (n = 10, 10 random yields were averaged in every experiment). *P<0.05; **P<0.01; ***P<0.001 (T-test). Scale bars: 50 μm (B, D, F).

FIGURE 2. *Rarg* and *Nr5a2* promote dendritic development of iN cells. *A*. Confocal reconstruction and quantification of dendrites of Map2a-positive cells 7 days post infection. From left to right, the images represent global dendritic form of iN cells converted from ABN neurons, ABN+CD437+DLPC neurons, and ABN+*Rarg*+*Nr5a2* neurons. *B*. Quantification of the ratio of unipolar, bipolar, and multipolar cells in iN cells. The values represent the mean ± SD. The numbers in the bars represent the total detected cell numbers. *C*. Quantification of the total branch length per cell of iN cells. *D*. Quantification of the total branch number per cell of iN cells. *E*. From left to right, the images show the single cell dendritic form of ABN neurons, ABN+CD437+DLPC neurons, and ABN+*Rarg*+*Nr5a2* neurons 2 weeks post infection. *F*. Quantification of the total branch length and number per cell of iN cells. *G*. Analysis of dendritic complexity of GFP+ neurons. Cumulative distribution plots of the total dendrite length and branch numbers are shown. Each symbol represents a single iN cell infected with ABN, ABN+CD437+DLPC, and ABN+*Rarg*+*Nr5a2*. The numbers in the bars represent the numbers of examined cells. The values represent the mean ± SEM. *P<0.05; **P<0.01; ***P<0.001 (T-test). Scale bars: 50 μm.

Downloaded from http://www.jbc.org/ by guest on April 28, 2020

FIGURE 3. *Rarg* and *Nr5a2* promote electrophysiological maturation of iN cells. Electrophysiology recordings were measured 7 days post infection. *A*. Representative traces showing whole-cell currents in voltage-clamp mode from iN cells. Cells were held at -70 mV; depolarization steps were applied from -80 mV to +60 mV at 10-mV intervals; the inset shows sodium currents. *B*. Representative traces showing action potentials in the current-clamp mode. The cells were maintained at a potential of approximately -65 mV. Step current injection was used from -50 to +70 pA. *C*, *D*. Na+ and K+ current crest values are shown for 7 days post infection. The numbers in the bars represent the numbers of detected cells. *E*-*H*. Analysis of membrane properties of iN cells in different groups. The numbers in the bars represent the numbers of recorded cells. The data are presented as the mean ± SEM. *P<0.05; **P<0.01; ***P<0.001 (T-test). AP, action potential; Cm, membrane capacitance; Rs, membrane series resistances; RMP, resting membrane potential. The action potential heights were measured from the baseline.

FIGURE 4. Characterization of *Rarg*- and *Nr5a2*-activated iN cells by neuron-specific staining and electrophysiological detection. *A*-*C*. At 7-12 days post-infection, ABN+*Rarg*+*Nr5a2* iN cells express the pan-neuronal markers Map2a (*A*), synapsin (*B*), and NeuN (*C*), along with Tuj1. *D*-*F*. After a longer culture period of 12-15 days, MEF-derived iN cells express a specific neuronal marker for excitatory neurons, vGLUT1 (*D*), a marker for inhibitory neurons, GAD67 (*E*), and a marker for dopaminergic neurons, TH (*F*). *G*-*K*. The iN cells were electrophysiologically recorded 12 days post infection ABN+CD437+DLPC. *G*. Representative traces of action potentials evoked by step-depolarization of the membrane in current-clamp mode. The membrane potential was current-clamped at approximately −65 mV. *H*. Representative traces of whole-cell currents in voltage-clamp mode. The lower panels show that iN cells were held at −55 mV, and step depolarization at 10-mV intervals was applied from −80 mV to +60 mV. The insets show sodium currents. *I*. iN cells show spontaneous action potentials. *J*. Map2a-positive iN cell coexpressed synapsin 12 days post infection. *K*. Representative spontaneous postsynaptic currents (PSCs) recorded from ABN+CD437+DLPC iN cells. *L*-*P*. The iN cells were electrophysiologically recorded 12 days post infection. The iN cells were converted by ABN+*Rarg*+*Nr5a2* iN cells. Scale bars: 20 μm.

FIGURE 5. *Rarg* and *Nr5a2* also promote the conversion of TTF to neurons. *A*-*C*. TTF-derived iN cells co-expressed the pan-neuronal markers Map2a (*A*), NeuN (*B*), and synapsin (*C*) 10 days post infection. *D*. Action potentials in response to step current injections of TTF-derived iN cells. E. Whole-cell currents recorded by step depolarization from −80 mV to 60 mV in TTF-derived iN cells. *F*-*H*. HEF-derived iN cells co-expressed the pan-neuronal markers Map2a (*F*), NeuN (*G*), and synapsin (*H*) 12 days post infection. I. Action potentials in response to step current injections of HEF-derived iN cells. J. Whole-cell currents recorded by step depolarization from −80 mV to 60 mV in HEF-derived iN cells.

Downloaded from http://www.jbc.org/ by guest on April 28, 2020

FIGURE 6. Transplantation of ABN+*Rarg*+*Nr5a2* iN cells in vivo. *A*, *E*. Schematic representation of iN cell transplantation and overview of grafted GFP+ cells in the brain cortex or dentate gyrus two weeks after transplantation. GFP (green), DAPI (blue). *B*, *F*, iN cells express the immature neuronal marker DCX one week after transplantation. *C*, *G*. iN cells express the mature neuronal marker NeuN two weeks after transplantation. *D*, *H*. iN cells express synapsin two weeks after transplantation. Scale bars: 50 μm (*A*, *E*), 10 μm (*B*-*D*, *F*-*H*).

FIGURE 7. Whole-genome gene expression profile and real-time PCR gene detection of iN cells. *A*. Hierarchical clustering analysis of global gene expression patterns of MEFs, iN cells, and primary neurons. Primary neurons were isolated from newborn pup hippocampus. iN cells were derived from MEFs after ABN+*Rarg*+*Nr5a2* conversion. A subset of differential genes was selected for clustering analysis. Group I and II are categorized as upregulated or downregulated genes compared with those in MEFs for both iN cells and primary neurons. The gene expression profile in iN cells is homoplastic to that in primary neurons. *B*. The functional gene categories associated with neurogenesis, neuron development, and synaptic formation are upregulated in iN cells and in primary neurons compared with MEFs. *C*. Real-time fluorescence quantification PCR shows that some neuronal-specificity genes are upregulated in iN cells, and the tendency is consistent to that in primary neurons.

Downloaded from http://www.jbc.org/ by guest on April 28, 2020

FIGURE 1

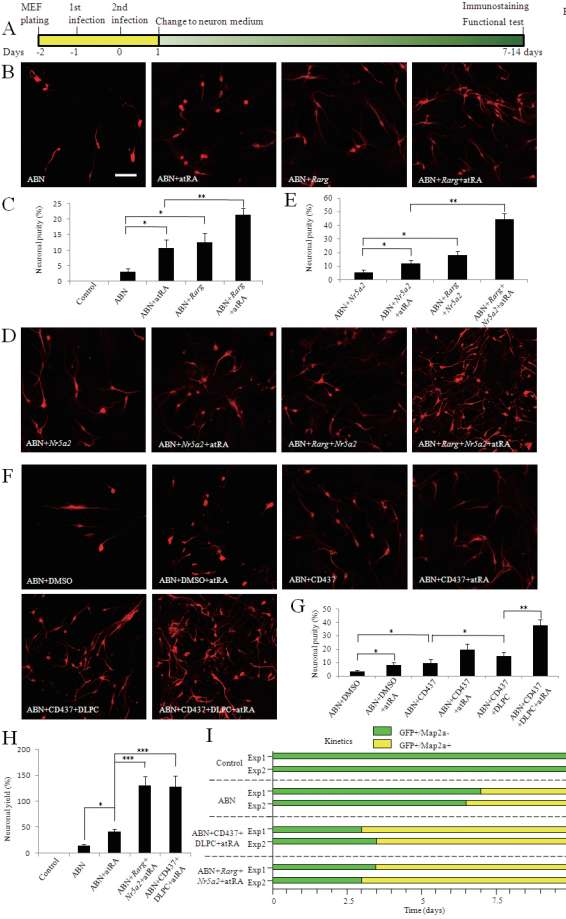
A
MEF plating
1st infection
2nd infection
Change to neuron medium
Immunostaining
Functional test
Days
-2
-1
0
1
7-14 days
B
ABN
ABN+atRA
ABN+Rarg
ABN+Rarg+atRA
C
Neuronal purity (%)
Control
ABN
ABN+atRA
ABN+Rarg
ABN+Rarg +atRA
E
ABN+Nr5a2
ABN+Nr5a2 +atRA
ABN+Rarg +Nr5a2
ABN+Rarg +Nr5a2+atRA
D
ABN+Nr5a2
ABN+Nr5a2+atRA
ABN+Rarg+Nr5a2
ABN+Rarg+Nr5a2+atRA
F
ABN+DMSO
ABN+DMSO+atRA
ABN+CD437
ABN+CD437+atRA
ABN+CD437+DLPC
ABN+CD437+DLPC+atRA
G
ABN+DMSO
ABN+DMSO +atRA
ABN+CD437
ABN+CD437 +atRA
ABN+CD437 +DLPC
ABN+CD437 +DLPC+atRA
H
Neuronal yield (%)
Control
ABN
ABN+atRA
ABN+Rarg +Nr5a2+atRA
ABN+CD437+ DLPC+atRA
I
Kinetics
GFP+/Map2a-
GFP-/Map2a+
Control
ABN
ABN+CD437+ DLPC+atRA
ABN+Rarg+ Nr5a2+atRA
Exp1
Exp2
Time (days)

FIGURE 2

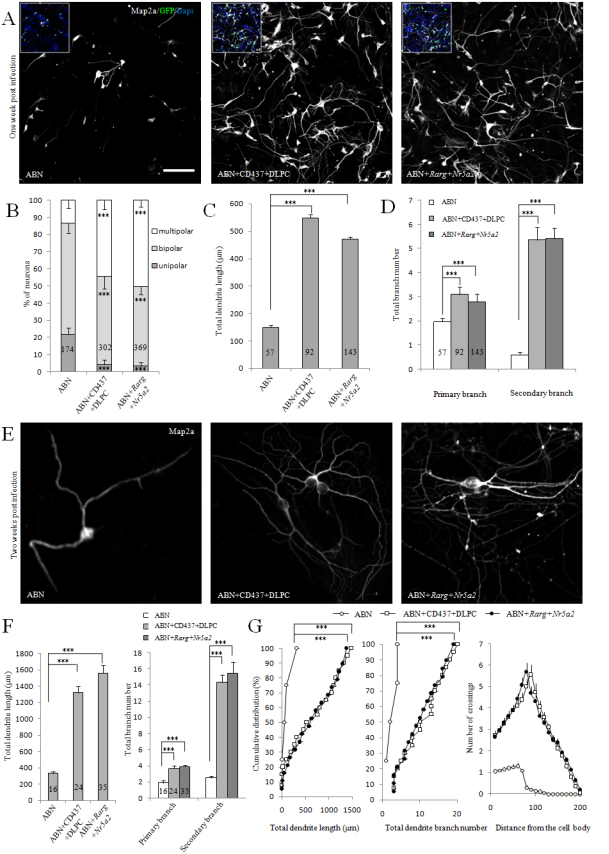
A
Map2a/GFP/Dapi
One week post infection
ABN
ABN+CD437+DLPC
ABN+Rarg+Nr5a2
B
% of neurons
multipolar
bipolar
unipolar
174
302
369
C
Total dendrite length (μm)
57
92
143
D
Total branch number
ABN
ABN+CD437+DLPC
ABN+Rarg+Nr5a2
Primary branch
Secondary branch
E
Map2a
Two weeks post infection
F
Total dendrite length (μm)
Total branch number
Primary branch
Secondary branch
G
Cumulative distribution(%)
Total dendrite length (μm)
Total dendrite branch number
Num ber of arcontage
Distance from the cell body

FIGURE 3

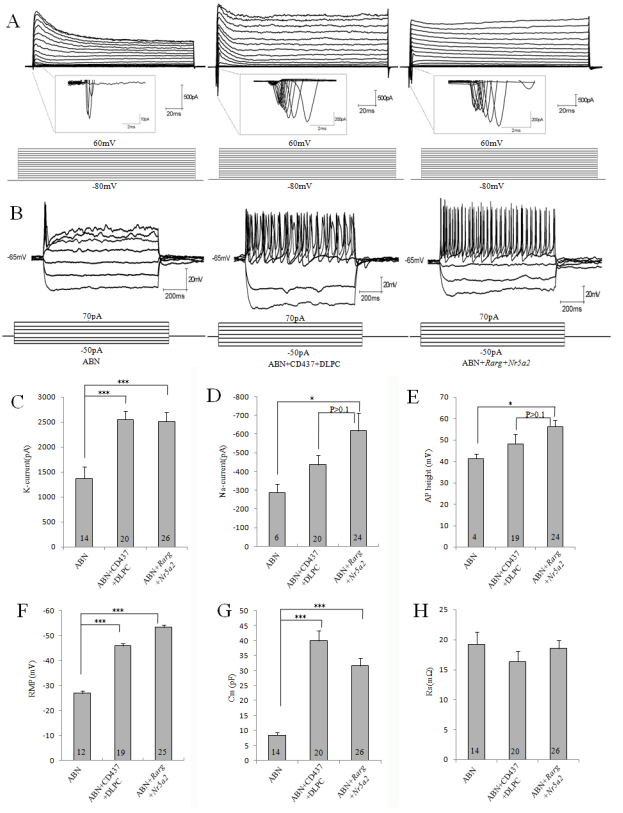
A
500pA
20ms
10pA
2ms
60mV
-80mV
B
-65mV
20mV
200ms
70pA
-50pA
ABN
ABN+CD437+DLPC
ABN+Rarg+Nr5a2
C
K+ current (pA)
D
Na+ current (pA)
P≥0.1
E
AP height (mV)
F
RMP (mV)
G
Cm (pF)
H
Rin (mΩ)
ABN
ABN+CD437 +DLPC
ABN+ Rarg +Nr5a2

FIGURE 4

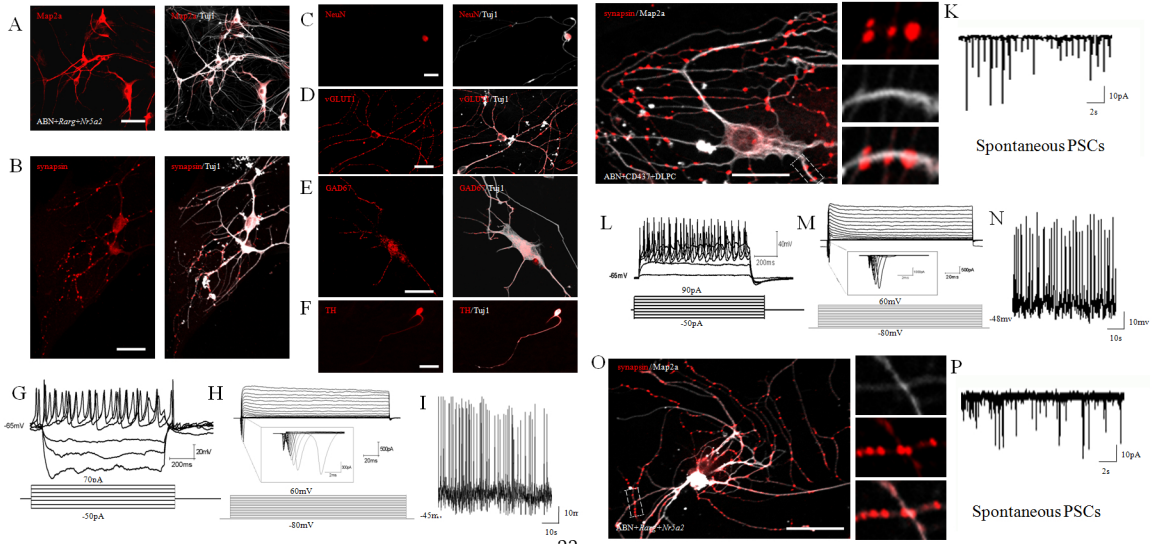
A
Map2a
Map2a/Tuj1
ABN+Rarg+Nr5a2
B
synapsin
synapsin/Tuj1
C
NeuN
NeuN/Tuj1
D
vGLUT1
vGLUT1/Tuj1
E
GAD67
GAD67/Tuj1
F
TH
TH/Tuj1
synapsin/Map2a
ABN+CD43+DLPC
K
10pA
2s
Spontaneous PSCs
L
-65mV
40mV
200ms
90pA
-50pA
M
60mV
-80mV
N
-48mv
10mv
10s
G
-65mV
20mV
200ms
70pA
-50pA
H
60mV
-80mV
I
-45m
10m
10s
O
synapsin/Map2a
ABN+Rarg+Nr5a2
P
10pA
2s
Spontaneous PSCs

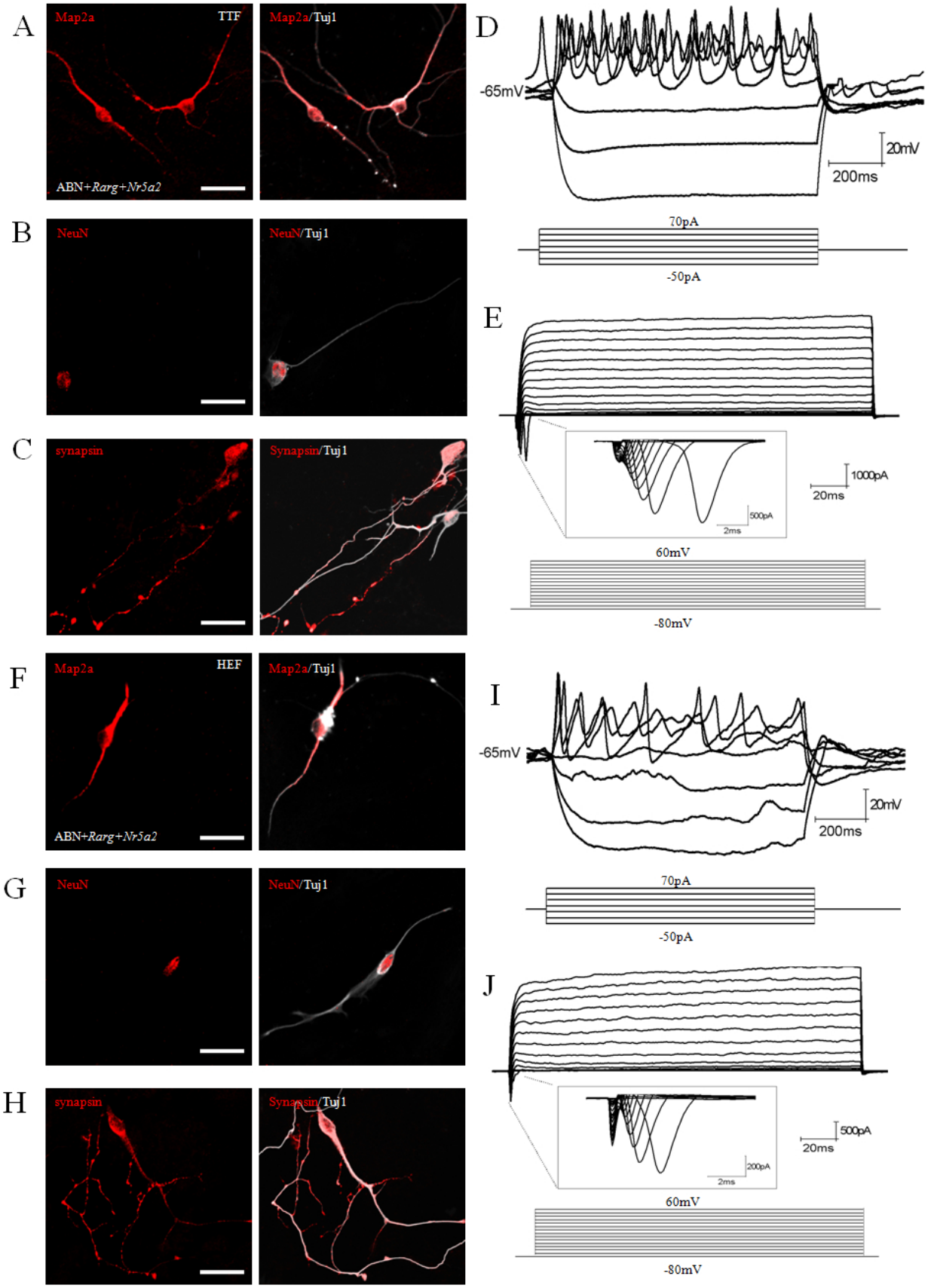
A
Map2a
TTF
Map2a/Tuj1
ABN+Rarg+Nr5a2
B
NeuN
NeuN/Tuj1
C
synapsin
Synapsin/Tuj1
D
-65mV
20mV
200ms
70pA
-50pA
E
1000pA
20ms
500pA
2ms
60mV
-80mV
F
Map2a
HEF
Map2a/Tuj1
ABN+Rarg+Nr5a2
G
NeuN
NeuN/Tuj1
H
synapsin
Synapsin/Tuj1
I
-65mV
20mV
200ms
70pA
-50pA
J
500pA
20ms
200pA
2ms
60mV
-80mV

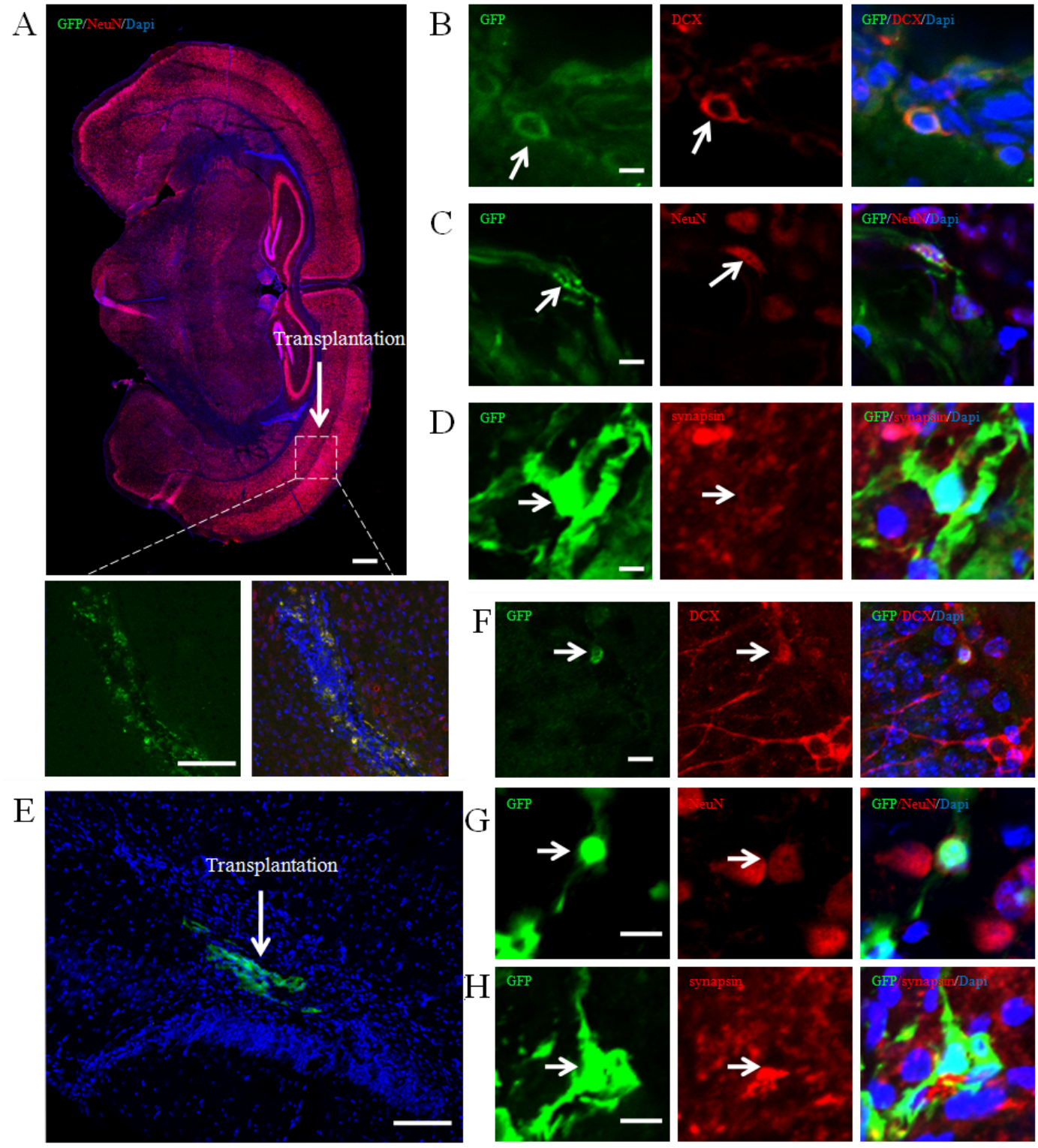
A
GFP/NeuN/Dapi
Transplantation
B
GFP
DCX
GFP/DCX/Dapi
C
GFP
NeuN
GFP/NeuN/Dapi
D
GFP
synapsin
GFP/synapsin/Dapi
E
Transplantation
F
GFP
DCX
GFP/DCX/Dapi
G
GFP
NeuN
GFP/NeuN/Dapi
H
GFP
synapsin
GFP/synapsin/Dapi

FIGURE 7

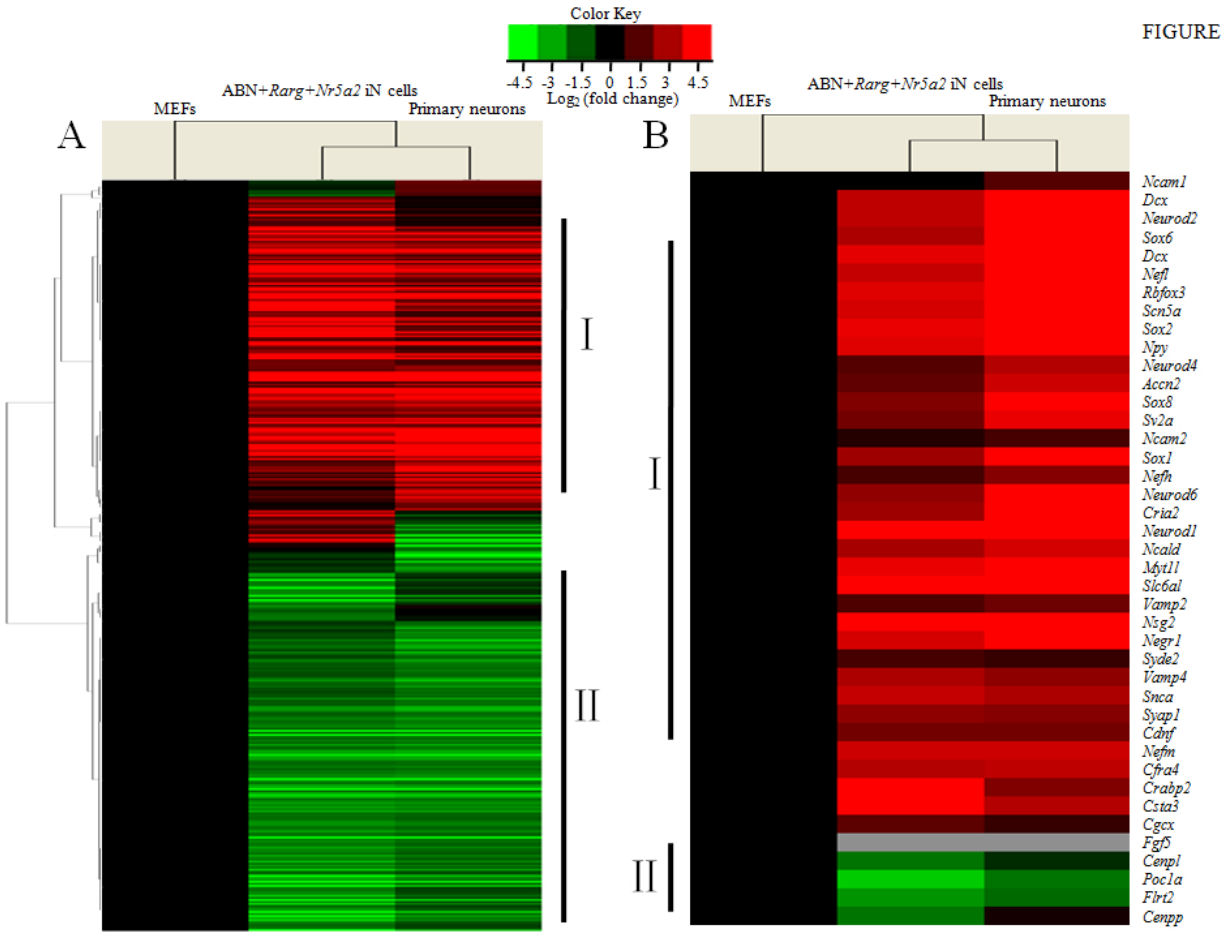
Color Key
-4.5 -3 -1.5 0 1.5 3 4.5
Log2 (fold change)
A
MEFs
ABN+Rarg+Nr5a2 iN cells
Primary neurons
I
II
B
MEFs
ABN+Rarg+Nr5a2 iN cells
Primary neurons
I
II
Ncam1
Dcx
Neurod2
Sox6
Dcx
Nefl
Rbfox3
Scn5a
Sox2
Npy
Neurod4
Accn2
Sox8
Sv2a
Ncam2
Sox1
Nefh
Neurod6
Cria2
Neurod1
Ncald
Myt1l
Slc6a1
Vamp2
Nsg2
Negr1
Syde2
Vamp4
Snca
Syap1
Cdnf
Nefm
Cfra4
Crabp2
Csta3
Cgcx
Fgf5
Cenpl
Poc1a
Flrt2
Cenpp

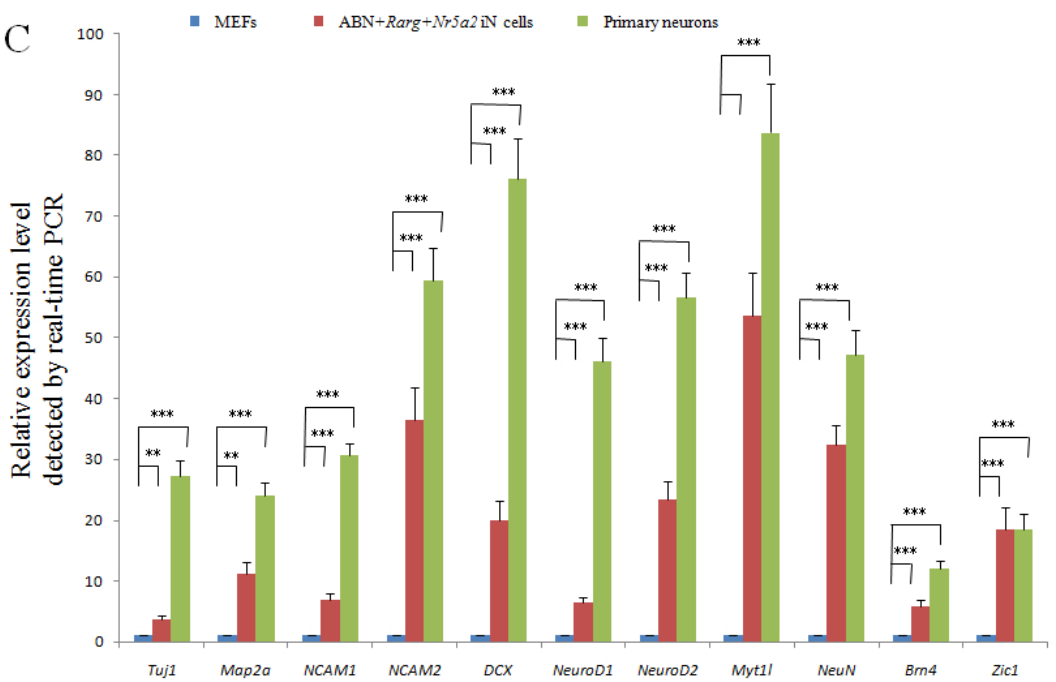
C
MEFs
ABN+Rarg+Nr5a2 iN cells
Primary neurons
Relative expression level detected by real-time PCR
0
10
20
30
40
50
60
70
80
90
100
Tuj1
Map2a
NCAM1
NCAM2
DCX
NeuroD1
NeuroD2
Myt1l
NeuN
Brn4
Zic1

Retinoic acid receptor gamma (Rarg) and nuclear receptor subfamily 5, group A, member 2 (Nr5a2) promote conversion of fibroblasts to functional neurons

Zixiao Shi, Tianjin Shen, Yanli Liu, Yuanyuan Huang and Jianwei Jiao

J. Biol. Chem. published online January 23, 2014

Access the most updated version of this article at doi: 10.1074/jbc.M113.515601

Alerts:
- When this article is cited
- When a correction for this article is posted

Click here to choose from all of JBC's e-mail alerts

Downloaded from http://www.jbc.org/ by guest on April 28, 2020